

RESEARCH ARTICLE

Correlation between various trace elements and ultramicroscopic structure of epiretinal macular membranes and glial cells

Mario R. Romano^{1*}, Gilda Cennamo², Daniela Montorio³, Salvatore Del Prete⁴, Mariantonio Ferrara³, Giovanni Cennamo³

1 Department of Biomedical Sciences, Humanitas University, Pieve Emanuele—Milan, Italy, **2** Department of Public Health, University Federico II, Naples, Italy, **3** Department of Neuroscience, Reproductive and Odontostomatological Science, University Federico II, Naples, Italy, **4** Interdepartment Electron Microscope Centre, University Federico II, Naples, Italy

* mario.romano.md@gmail.com



Abstract

Introduction

Elements such as zinc, iron, copper, sulphur and phosphorus have been identified in retinal layers and implicated in vital retinal functions. Regarding mineral composition of epiretinal membranes (ERMs), literature is lacking. This study aimed to analyze both mineral composition and anatomical ultrastructure of ERMs to clarify the pathophysiology of this disease.

Methods

Twenty ERMs (10 diabetic ERMs and 10 idiopathic ERMs) from 20 patients were harvested during pars plana vitrectomy. Scanning Electron Microscopy (SEM) was used to investigate the anatomical ultrastructure of the peeled ERMs. Mineral composition was analyzed using energy-dispersive spectrometry (EDS). The most frequent elements were evaluated in relation to appearance of ERMs analyzed at SEM and at OCT images.

Results

Sulphur was the most frequent element found (in 80% of the samples), followed by sodium (50%) and phosphorus (45%). The presence of these elements was not significantly different between diabetic and idiopathic ERMs ($P > 0.05$). Using SEM we found a folded tissue in all ERMs, except in 4 ERMs, where we observed only a smooth tissue. There was a trend of sodium to be more frequent in ERMs with folded layers at SEM examination.

Conclusions

Several elements were identified in ERMs, and sulphur, sodium and phosphorus were the most frequent ones. This finding may help to understand their role in the physiopathology of epiretinal proliferation and in glial activation.

OPEN ACCESS

Citation: Romano MR, Cennamo G, Montorio D, Del Prete S, Ferrara M, Cennamo G (2018) Correlation between various trace elements and ultramicroscopic structure of epiretinal macular membranes and glial cells. PLoS ONE 13(9): e0204497. <https://doi.org/10.1371/journal.pone.0204497>

Editor: Demetrios G. Vavvas, Massachusetts Eye & Ear Infirmary, Harvard Medical School, UNITED STATES

Received: February 15, 2018

Accepted: September 10, 2018

Published: September 28, 2018

Copyright: © 2018 Romano et al. This is an open access article distributed under the terms of the [Creative Commons Attribution License](https://creativecommons.org/licenses/by/4.0/), which permits unrestricted use, distribution, and reproduction in any medium, provided the original author and source are credited.

Data Availability Statement: All relevant data are within the manuscript.

Funding: The authors received no specific funding for this work.

Competing interests: The authors have declared that no competing interests exist.

Introduction

Epiretinal membrane (ERM) is the most common type of fibrocellular proliferation at the vitreoretinal interface and is significantly associated with aging [1–3].

Several previous studies aimed to identify the cell types in ERMs using light and electron microscopy [4–8]. However, during the last decades, morphologic analyses of surgically excised ERM specimens were inadequate because of the phenotypic trans-differentiation of proliferating epiretinal cells [9–11]. Showing the presence of glial cells (Muller cells, fibrous astrocytes, microglia), fibroblasts, myofibroblasts, hyalocytes, retinal pigment epithelial cells and macrophages, recent immunohistochemical investigations confirmed the involvement of these cells in ERM formation [12–14].

Recently Azzolini et al. [15] observed the appearance of iERMs at scanning electron microscopy (SEM), identifying four types of structures distributed in various layers from ILM to vitreous side of the membranes. In particular, the Authors described: (a) thin layers of woven fibers; (b) folded layers of fibrous material; (c) rigid, thicker and more densely folded layers of collagen fibrils; and (d) necrotic and/or inflammatory material in lacunar structures.

Previous studies investigated the presence of mineral elements in the retinal layers because of their role in various retinal diseases [16]. It has been demonstrated that the altered homeostasis of zinc and iron is implicated in retinal dysfunction and age-related macular degeneration [17–18], as well as copper deficiency in optic neuropathy and altered zinc levels in poor dark adaptation [17].

As far as we know, in literature there is no study regarding mineral composition of ERMs.

Our purpose is to investigate both anatomical ultrastructure and mineral composition of ERMs, in order to improve the understanding of the pathophysiology of this disease.

Materials and methods

In this prospective study we evaluated 20 ERMs of 20 consecutive patients enrolled in the Eye Clinic of the University of Naples “Federico II” from July to October 2016. Before undergoing surgery, all patients signed a written informed consent. The study was approved by the Institutional Review Board of the University of Naples “Federico II” and all investigations adhered to the tenets of the Declaration of Helsinki. We included 10 idiopathic ERMs (iERMs) and 10 ERMs secondary to diabetic retinopathy (dERMs). Exclusion criteria were previous ophthalmic laser and surgical treatment, intravitreal injection, vascular occlusions, inflammatory eye diseases, history of ocular trauma and significant ocular media opacities precluding an adequate fundus and optical coherence tomography (OCT) examination.

All patients underwent best corrected visual acuity (BCVA) test by Snellen eye chart, slit-lamp biomicroscopy, dilated fundus examination, Spectral Domain-OCT by RTVue-100 OCT XR Avanti (Optovue Inc., Fremont, CA, USA; software version 4.0.5.39) and Spectralis OCT (Heidelberg Engineering, Heidelberg, Germany) with multimodal imaging. Based on fundus examination, multicolor and infrared images, we categorized ERMs according Gass’s classification. (REF)

The 20 eyes underwent 25-gauge pars plana vitrectomy and ERM peeling dye-assisted.

Immediately after their removal, ERM specimens were fixed in 3% glutaraldehyde in a 0.065 M (pH 7.4) phosphate buffer for two hours at room temperature. Slides were washed three times in 0.065 M phosphate buffer (for 30 minutes), then placed in 1% OsO₄ in 0.065 M (pH 7.4) phosphate buffer for 30 minutes. The samples were dehydrated through a graded series of ethanol, and then critical-point-dried in a CO₂ liquid Bemar SPC 1500 apparatus (Bomar Co, Tacome, WA, USA). Specimens were mounted on aluminium stubs, placed into molecular coating with graphite and examined using SEM JEOL (JSM 5310).

Mineral composition was analysed using energy-dispersive X-ray spectrometry (EDS) with an EDS detector (Oxford Instruments-INCA). Qualitative EDS analysis was performed using the 'automatic peak identification' software. When invoked, automatic peak identification applies a mathematical algorithm to locate and measure the photon energy of the characteristic peaks in the spectrum and then assigns elemental labels from a database of elemental X-ray energy information [19]. The slides and the dyes were also analyzed EDS in order to exclude any interference in mineral evaluation of ERMs.

Statistical analysis

Statistical analysis was performed using the Statistical Package for Social Sciences (Version 20.0 for Windows; SPSS Inc, Chicago, Ill, USA). The Fisher's exact test was used to evaluate if the difference in the presence of the most frequent elements was significant between iERMs and dERMs. A p value < 0.05 was considered statistically significant.

Results

Twenty ERMs surgically removed from 20 eyes of 20 patients (10 females and 10 males) were examined. The mean age was 65.5 ± 9.77 years and the mean preoperative BCVA was 0.66 ± 0.18 logMAR. Ten of 20 patients were affected by dERM and 10 by iERM.

All ERMs were classified according to Gass's criteria [1]: 65% was grade I (6 dERMs, 7 iERMs); 35% grade II (4 dERMs, 3 iERMs).

We observed all ERMs at SEM. According to the structures recently described by Azzolini et al. [15], we found a smooth appearance due to only thin layers of woven fibers in 4 ERMs (2 dERMs, 2 iERMs) and folded tissue in all the remaining thicker membranes (Figs 1 and 2). All grade II ERMs showed a folded structure at SEM.

Using qualitative SEM/EDS analysis, we identified 15 elements. Of these, aluminium, carbon, and osmium were excluded, because of their presence on the slides. Sulphur was the most frequent element, as it was found in 80% of the samples (9 dERMs and 7 iERMs), followed by sodium (50%, 6 dERMs and 4 iERMs) and phosphorus (45%, 6 dERMs and 3 iERMs) (Figs 1 and 2). The remaining nine elements (silicon, iron, calcium, potassium, magnesium, iodine, manganese, bromine and titanium) were less frequent (Table 1).

No statistically significant difference was found between the percentage of sulphur, sodium and phosphorus in diabetic versus idiopathic ERMs ($P > 0.05$).

The number of cases with smooth appearance at SEM was too small to assess any statistically significant difference in the distribution of different elements, when compared with the remaining ERMs. However, we found a trend of sodium to be more frequent in ERMs characterized by folded layers at SEM examination, accounting for the 90% of the ERMs in which the sodium was detected.

Discussion

To our knowledge, this is the first study analyzing both the mineral composition and anatomical ultrastructure in ERMs using SEM/EDS.

Previous studies examined the cellular layers of ERMs, using tissue cultures and SEM in order to detect the cellular phenotypes involved in the formation of these membranes [20,21]. In particular, recently Azzolini et al. identified different layers of various materials in iERMs [15].

Our study showed a novel finding: the sulphur is the most frequent element in the ERMs. This element is known to be present in significant amounts in proteins, as component of cysteine and methionine [22]. The detection of sulphur may be attributed to the several proteins

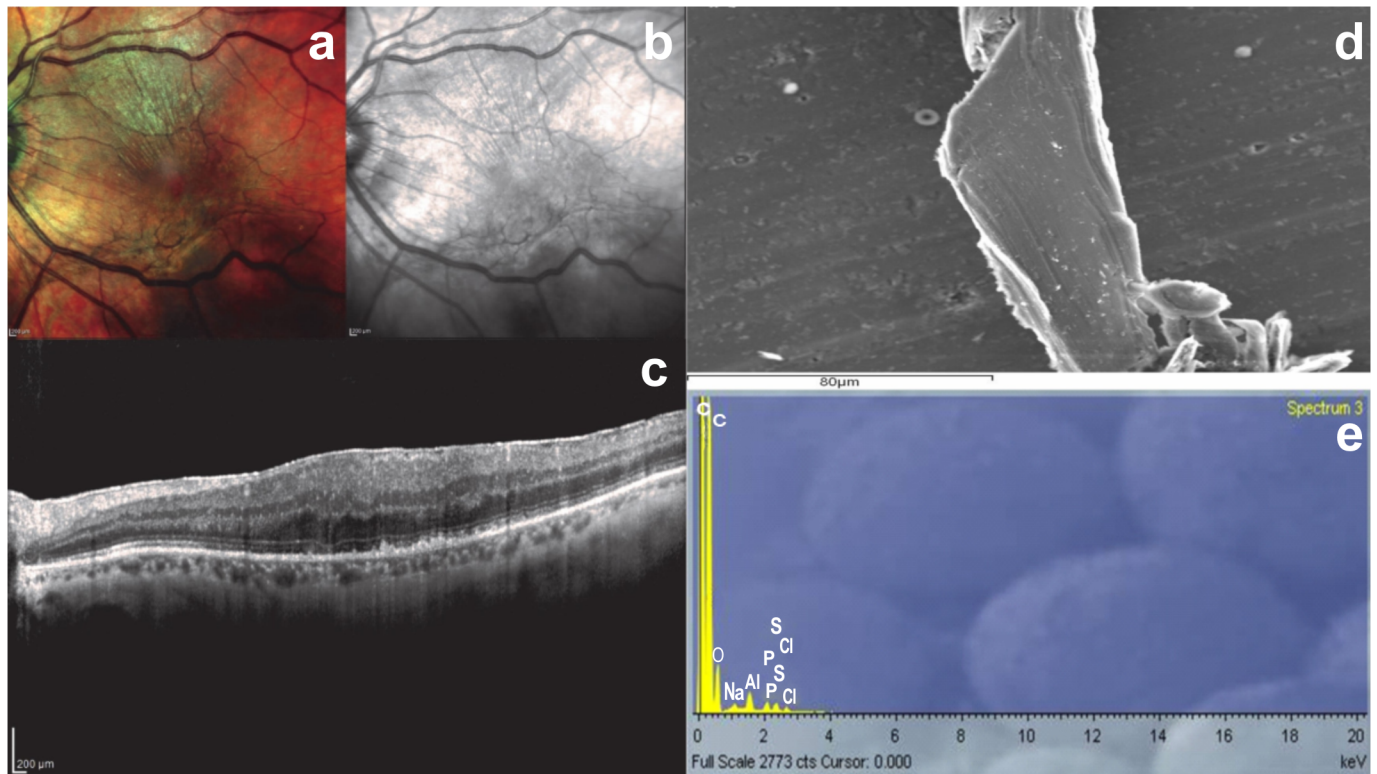


Fig 1. Analysis of a sample ERM with smooth appearance at SEM. a-c) Multicolor image, infrared and structural OCT B-scan showing slight epiretinal proliferation; d) Scanning electron microscope sample revealing smooth tissue; e) SEM/EDS analysis showing the mineral composition of the sample: sulphur, sodium and phosphorus are the most frequent elements.

<https://doi.org/10.1371/journal.pone.0204497.g001>

involved in the pathophysiology of ERMs. First, glial fibrillary acidic protein (GFAP), a specific intermediate filament protein. Indeed, previous studies have demonstrated that glial cells, in particular Müller cells, were the predominant cell type in ERMs [12] and GFAP is the main component of their cytoskeleton [23]. Moreover, GFAP is overexpressed as consequence of damage or stress to the retina, including ERM [24–29]. Second, fibronectin, laminin and vitronectin, that are glycoproteins of the extracellular matrix. These proteins are involved in ERM formation (cellular adhesion, migration, and phenotype differentiation at the vitreoretinal interface) and contain disulfide bonds [30,31]. Third, secreted proteins acidic and rich in cysteine: SPARCs, glycoproteins with adhesive functions located on the basal surface of RPE cells [32,33]. During ERM development, SPARCs reduce the adhesion between RPE and Bruch’s membrane, allowing RPE cells to migrate to the vitreoretinal interface where they de-differentiate into a fibroblast-like cells [34]. At last, metallothioneins, cysteine-rich proteins over-produced by the retina under oxidative stress conditions and involved in ERM formation [7–9].

In this study, the sodium was detected in 50% of samples, mainly in the thicker ERMs (with folded tissue at SEM examination). Recent studies demonstrated that Na^+ pumps and Na^+ -dependent ion transporters in astrocytes, microglia and oligodendrocytes regulate Na^+ homeostasis, modulating glia activity in both physiological conditions and neurological diseases [35–37]. Moreover, Na^+ signalling increases as consequence of tissue damage [38]. After the ERM formation, in response to chronic insults, such as increased oxidative stress, Na^+ signalling may contribute to glial activation, cell migration, and gliosis determining the further

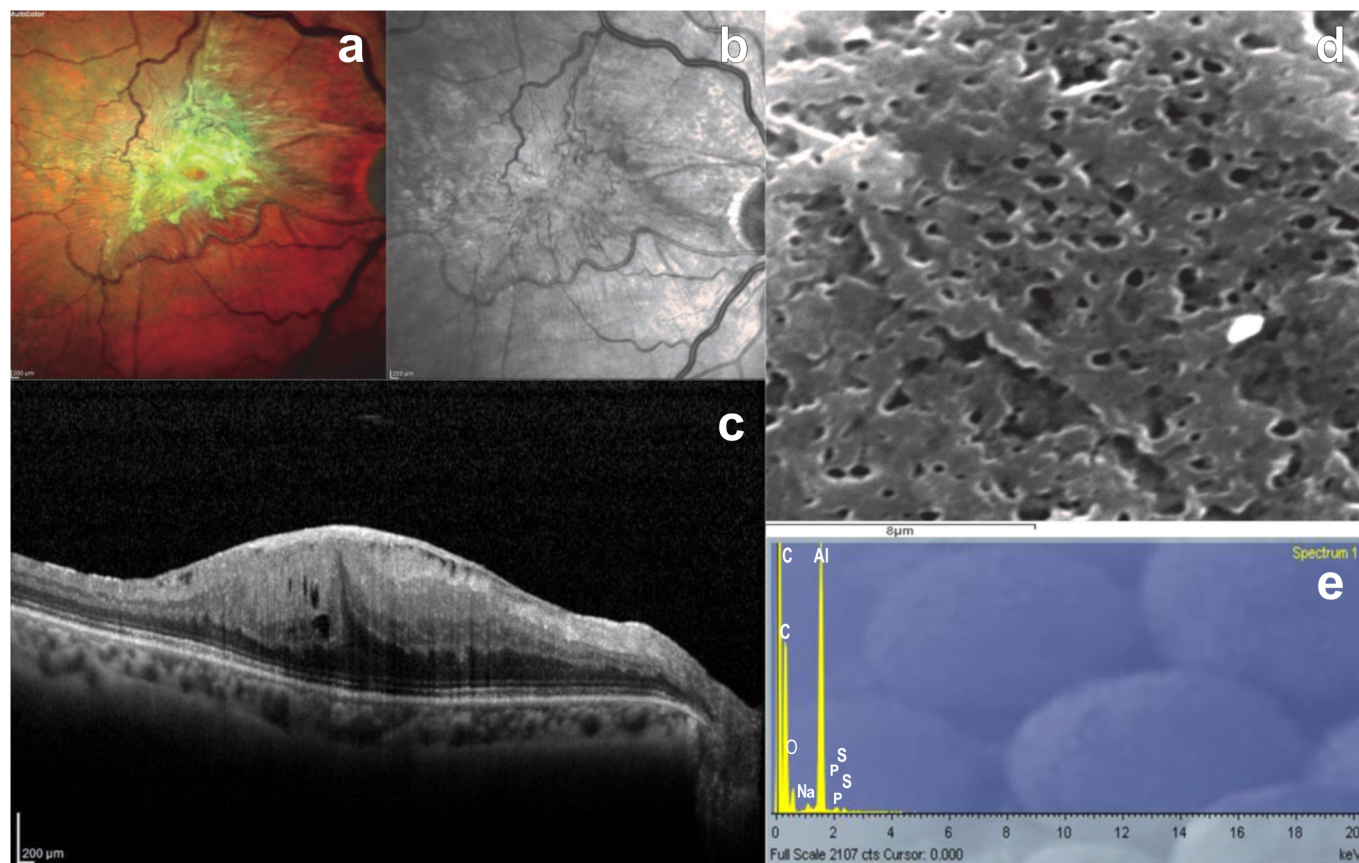


Fig 2. Analysis of a sample ERM with folded appearance at SEM. a-c) Multicolor image, infrared and structural OCT B-scan showing significant epiretinal proliferation; d) Scanning electron microscope sample revealing fibrotic folded tissue; e) SEM/EDS analysis showing the mineral composition of the sample: sulphur, sodium and phosphorus are the most frequent elements.

<https://doi.org/10.1371/journal.pone.0204497.g002>

development of ERMs. This process may explain the higher detection of sodium in thicker ERMs.

Table 1. Percentage of frequency of different elements in ERMs.

Element	Frequency of detection
Sulphur (S)	80%
Sodium (Na)	50%
Posphorus (P)	45%
Silicon (Si)	20%
Calcium (Ca)	10%
Iron (I)	10%
Potassium (K)	5%
Magnesium (Mg)	5%
Manganese (Mn)	5%
Iodine (I)	5%
Bromine (Br)	5%
Titanium (Ti)	5%

<https://doi.org/10.1371/journal.pone.0204497.t001>

Lastly, the phosphorus was found in 45% of ERMs. This finding may be attributed to the activation and proliferation of Muller cells, that need high amount of adenosine 5' triphosphate (ATP) for DNA synthesis [39,40]. The phosphorus is the main component of ATP.

The main limitation of this study is the small sample size.

In conclusion, our study identified traces of several elements in ERMs, a useful and interesting finding to understand their functional role in the physiopathology of this disease and, particularly, in glial activation.

Author Contributions

Formal analysis: Gilda Cennamo.

Methodology: Salvatore Del Prete.

Project administration: Mariantonia Ferrara.

Supervision: Giovanni Cennamo.

Writing – original draft: Daniela Montorio.

Writing – review & editing: Mario R. Romano.

References

1. Gass JDM. Stereoscopic atlas of macular diseases. 4th ed. St. Louis, MO: Mosby; 1997.
2. Bu S.C, Kuijjer R, Li X.R, Hooymans J.M, Los L.I. Idiopathic epiretinal membrane. *Retina*. 2014; 34: 2317–2335. <https://doi.org/10.1097/IAE.0000000000000349> PMID: 25360790
3. Heidenkummer H.P, Kampik A. Morphologic analysis of epiretinal membranes in surgically treated idiopathic macular foramina. Results of light and electron microscopy. *Ophthalmologie*. 1996; 93: 675–679. PMID: 9081523
4. Kampik A, Kenyon KR, Michels R.G, Green WR, de la Cruz ZC. Epiretinal and vitreous membranes. Comparative study of 56 cases. *Arch Ophthalmol*. 1981; 99: 1445–1454. PMID: 7020665
5. Schumann R.G, Schaumberger M.M, Rohleder M, Haritoglou C, Kampik A, Gandorfer A. Ultrastructure of the vitreomacular interface in full-thickness idiopathic macular holes: a consecutive analysis of 100 cases. *Am J Ophthalmol*. 2006; 141: 1112–1119. <https://doi.org/10.1016/j.ajo.2006.01.074> PMID: 16765681
6. Gandorfer A, Rohleder M, Grosselfinger S, Haritoglou C, Ulbig M, Kampik A. Epiretinal pathology of diffuse diabetic macular edema associated with vitreomacular traction. *Am J Ophthalmol*. 2005; 139: 638–652. <https://doi.org/10.1016/j.ajo.2004.11.035> PMID: 15808159
7. Yooh HS, Brooks HL Jr, Capone A Jr, L'Hernault NL, Grossniklaus HE. Ultrastructural features of tissue removed during idiopathic macular hole surgery. *Am J Ophthalmol*. 1996; 122: 67–75. PMID: 8659600
8. Armstrong D, Augustin AJ, Spengler R, Al-Jada A, Nickola T, Grus F, et al. Detection of vascular endothelial growth factor and tumor necrosis factor alpha in epiretinal membranes of proliferative diabetic retinopathy, proliferative vitreoretinopathy and macular pucker. *Ophthalmologica*. 1998; 212: 410–414. <https://doi.org/10.1159/000027378> PMID: 9787233
9. Viores SA, Campochiaro PA, McGehee R, Orman W, Hackett SF, Hjelmeland LM. Ultrastructural and immunocytochemical changes in retinal pigment epithelium, retinal glia, and fibroblasts in vitreous culture. *Invest Ophthalmol Vis Sci*. 1990; 31: 2529–2545. PMID: 1702409
10. Viores SA, Campochiaro PA, Conway BP. Ultrastructural and electron-immunocytochemical characterization of cells in epiretinal membranes. *Invest Ophthalmol Vis Sci*. 1990; 31: 14–28. PMID: 1688833
11. Nishimura H, Nishimura N, Kobayashi S, Tohyama C. Immunohistochemical localization of metalloproteinase in the eye of rats. *Histochemistry*. 1991; 95: 535–539. PMID: 1856106
12. Schumann R.G, Eibl KH, Zhao F, Scheerbaum M, Scheler R, Schaumberger M.M, et al. Immunocytochemical and ultrastructural evidence of glial cells and hyalocytes in internal limiting membrane specimens of idiopathic macular holes. *Invest Ophthalmol Vis Sci*. 2011; 52: 7822–7834. <https://doi.org/10.1167/iovs.11-7514> PMID: 21900375
13. Zhao F, Gandorfer A, Haritoglou C, Scheler R, Schaumberger M.M, Kampik A, et al. Epiretinal cell proliferation in macular pucker and vitreomacular traction syndrome: analysis of flat-mounted internal limiting

- membrane specimens. *Retina*. 2013; 33: 77–88. <https://doi.org/10.1097/IAE.0b013e3182602087> PMID: 22914684
14. Higashimori H, Sontheimer H. Role of Kir4.1 channels in growth control of glia. *Glia*. 2007; 55: 1668–1679. <https://doi.org/10.1002/glia.20574> PMID: 17876807
 15. Ugarte M, Grime GW, Lord G, Geraki K, Collingwood JF, Finnegan M.E, et al. Concentration of various trace elements in the rat retina and their distribution in different structures. *Metallomics*. 2012; 4: 1245–1254. <https://doi.org/10.1039/c2mt20157g> PMID: 23093062
 16. Ugarte M, Osborne NN, Brown LA, Bishop PN. Iron, zinc, and copper in retinal physiology and disease. *Surv Ophthalmol*. 2013; 58: 585–609. <https://doi.org/10.1016/j.survophthal.2012.12.002> PMID: 24160731
 17. Erie JC, Good JA, Butz JA, Pulido JS. Reduced zinc and copper in the retinal pigment epithelium and choroid in age-related macular degeneration. *Am J Ophthalmol*. 2009; 147: 276–282. <https://doi.org/10.1016/j.ajo.2008.08.014> PMID: 18848316
 18. Newbury DE, Ritchie NW. Is scanning electron microscopy/energy dispersive X-ray spectrometry (SEM/EDS) quantitative? *Scanning*. 2013; 35: 141–68. <https://doi.org/10.1002/sca.21041> PMID: 22886950
 19. Hiscott PS, Grierson I, Hitchins CA, Rahi AH, McLeod D. Epiretinal membranes in vitro. *Trans Ophthalmol Soc UK*. 1983; 103: 89–102. PMID: 6362111
 20. Mazure A, Grierson I. In vitro studies of the contractility of cell types involved in proliferative vitreoretinopathy. *Invest Ophthalmol Vis Sci*. 1992; 3: 3407–3416.
 21. Azzolini C, Congiu T, Donati S, Passi A, Basso P, Piantanida E, et al. Multilayer microstructure of idiopathic epiretinal macular membranes. *Eur J Ophthalmol*. 2017; 19: 0. <https://doi.org/10.5301/ejo.5000982> PMID: 28525683
 22. Brosnan JT, Brosnan ME. The sulfur-containing amino acids: an overview. *J Nutr*. 2006; 136:1636S–1640S. <https://doi.org/10.1093/jn/136.6.1636S> PMID: 16702333
 23. Joshi M, Agrawal S, Christoforidis JB. Inflammatory mechanisms of idiopathic epiretinal membrane formation. *Mediators Inflamm*. 2013; 2013:192582. <https://doi.org/10.1155/2013/192582> PMID: 24324293
 24. Lewis GP, Fisher SK. Up-regulation of glial fibrillary acidic protein in response to retinal injury: its potential role in glial remodeling and a comparison to vimentin expression. *Int Rev Cytol*. 2003; 230: 263–290. PMID: 14692684
 25. Erickson PA, Fisher SK, Guerin CJ, Anderson DH, Kaska DD. Glial fibrillary acidic protein increases in Muller cells after retinal detachment. *Exp Eye Res*. 1987; 44: 37–48. PMID: 3549345
 26. Lewis GP, Guerin CJ, Anderson DH, Matsumoto B, Fisher SK. Rapid changes in the expression of glial cell proteins caused by experimental retinal detachment. *Am J Ophthalmol*. 1994; 118: 368–376. PMID: 7916177
 27. Hiscott PS, Grierson I, Trombetta CJ, Rahi AH, Marshall J, McLeod D. Retinal and epiretinal glia—an immunohistochemical study. *Br J Ophthalmol*. 1984; 68: 698–707. PMID: 6383462
 28. Kenawy N, Wong D, Stappler T, Romano MR, Das RA, Hebbar G, et al. Does the presence of an epiretinal membrane alter the cleavage plane during internal limiting membrane peeling? *Ophthalmology*. 2010; 117: 320–323. <https://doi.org/10.1016/j.ophtha.2009.07.024> PMID: 20006906
 29. Charteris DG, Downie J, Aylward GW, Sethi C, Luthert P. Intraretinal and periretinal pathology in anterior proliferative vitreoretinopathy. *Graefes Arch Clin Exp Ophthalmol*. 2007; 245: 93–100. <https://doi.org/10.1007/s00417-006-0323-5> PMID: 16612635
 30. Casaroli Marano R.P, Vilaró S. The role of fibronectin, laminin, vitronectin and their receptors on cellular adhesion in proliferative vitreoretinopathy. *Invest Ophthalmol Vis Sci*. 1994; 35: 2791–2803.
 31. Grisanti S, Heimann K, Wiedemann P. Origin of fibronectin in epiretinal membranes of proliferative vitreoretinopathy and proliferative diabetic retinopathy. *Br. J. Ophthalmol*. 1993; 77: 238–242. PMID: 8494861
 32. Hiscott P, Hagan S, Heathcote L, Sheridan CM, Groenewald CP, Grierson I, et al. Pathobiology of epiretinal and subretinal membranes: possible roles for the matricellular proteins thrombospondin 1 and osteonectin (SPARC). *Eye (Lond)*. 2002; 16: 393–403.
 33. Scavelli K, Chatterjee A, Rhee DJ. Secreted Protein Acidic and Rich in Cysteine in Ocular Tissue. *J Ocul Pharmacol Ther*. 2015; 31: 396–405. <https://doi.org/10.1089/jop.2015.0057> PMID: 26167673
 34. Grierson I, Hiscott P, Hogg P, Robey H, Mazure A, Larkin G. Development, repair and regeneration of the retinal pigment epithelium. *Eye (Lond)*. 1994; 8: 255–62.
 35. Rose CR, Chatton JY. Astrocyte sodium signaling and neuro-metabolic coupling in the brain. *Neuroscience*. 2016; 26: 121–134. <https://doi.org/10.1016/j.neuroscience.2015.03.002> PMID: 25791228

36. Rose CR, Karus C. Two sides and of the same coin: Sodium homeostasis and signaling in astrocytes under physiological and pathophysiological conditions. *Glia*. 2013; 61: 1191–1205. <https://doi.org/10.1002/glia.22492> PMID: [23553639](https://pubmed.ncbi.nlm.nih.gov/23553639/)
37. Rose C.R, Verkhratsky A. Principles of sodium homeostasis and sodium signalling in astroglia. *Glia*. 2016; 64: 1611–1627. <https://doi.org/10.1002/glia.22964> PMID: [26919326](https://pubmed.ncbi.nlm.nih.gov/26919326/)
38. Boscia F, Begum G, Pignataro G, Sirabella R, Cuomo O, Casamassa A, et al. Glial Na⁽⁺⁾-dependent ion transporters in pathophysiological conditions. *Glia*. 2016; 64: 1677–1697. <https://doi.org/10.1002/glia.23030> PMID: [27458821](https://pubmed.ncbi.nlm.nih.gov/27458821/)
39. Moll V, Weick M, Milenkovic I, Kodal H, Reichenbach A, Bringmann A. P2Y receptor-mediated stimulation of Müller glial DNA synthesis. *Invest Ophthalmol Vis Sci*. 2002; 43: 766–773. PMID: [11867596](https://pubmed.ncbi.nlm.nih.gov/11867596/)
40. Kodal H, Weick M, Moll V, Biedermann B, Reichenbach A, Bringmann A. Involvement of calcium-activated potassium channels in the regulation of DNA synthesis in cultured Müller glial cells. *Invest Ophthalmol Vis Sci*. 2000; 41: 4262–4267. PMID: [11095624](https://pubmed.ncbi.nlm.nih.gov/11095624/)